Macromolecules

ARTICLE

pubs.acs.org/Macromolecules

Phase Behavior of Disk−Coil Macromolecules

YongJoo Kim, Edward Ha, and Alfredo Alexander-Katz*

Department of Materials Science and Engineering, Massachusetts Institute of Technology, Cambridge, Massachusetts 02139, United States

ABSTRACT: We explore the self-assembly of disk−coil macromolecules using Monte Carlo simulations in the NPT ensemble. Our study focuses on the role that coil length compared to the size of the disk has on the phase behavior of the system as well as the effect of added stacking interactions between the disks. As a function of temperature T, we find a disordered phase at high T and lamellar, perforated lamellar, and cylinder phases with liquidlike correlations at intermediate T. If we further lower the temperature, the disk-rich regions spontaneously order, and we find ordered lamellar, ordered perforated lamellar, and ordered cylinder phases depending on the strength of the stacking interactions. The appearance of any of these phases is, however, strongly dependent on the length of the coil with respect to the diameter of the disk. In addition to constructing a comprehensive phase diagram, we further analyze the correlations in the system, as well as the director vector field of the disks, and use it to construct an order parameter. We show that the latter changes drastically at the ordering transition points. We find that the ordered cylinder phase has a high degree of parallel packing. Our results are important to understand the self-assembly of supramolecular structures of disk−coil amphiphiles that are ubiquitous in nature, such as the chlorophyll molecule.

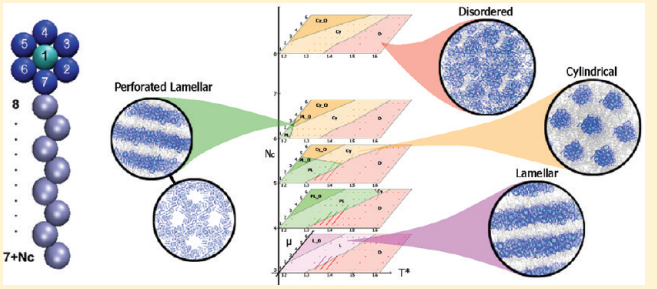

1. INTRODUCTION

Planar organic macromolecules have been an important area of research during the past decades and have become extremely relevant in recent years due to their applications in diverse fields such as organic electronics,[1,2] catalysis,[3,4] and organic photovoltaics.[5] These molecules are typically composed of highly conjugated cores that have relatively strong attractive stacking interactions which make them hard to process. In order to make them processable, they need to be decorated with alkyl (coil-like) chains on their periphery. The functionalization also helps during the self-assembly process because the system is "funneled" into ordered structures since all the metastable states appearing in the pure disk phase are removed.[6,7] Using multiple alkyl chains to functionalize the disks has been the standard in the field due to facile synthesis, but other functionalizations in which only one coil is present are possible.[8,9] Nature, for example, uses a disk−coil molecule, chlorophyll, for all photosynthetic apparatuses. Although in higher organisms this molecule is templated by specialized proteins to form light harvesting complexes, some bacteria rely on the self-assembly of this molecule by itself to create highly efficient light harvesting antennas called chlorosomes.[10−14] In this article we investigate the phase behavior of such disk−coil systems, and in particular we focus on (i) the role of the difference between the diameter of disk and the length of the coil has on the phase behavior and (ii) the effect of the stacking interactions between the disks. We use a minimal model in order to extract the important features of the system. Our results are important to understand the ordered phases of disk−coil amphiphiles, a common motif in synthetic and biological macromolecules.

Multiscale simulations of molecules with multiple alkyl tails have shown that it is possible to create highly ordered columnar phases.[15−19] However, until recently the single coil problem had not been treated, despite the wider range of structures that are

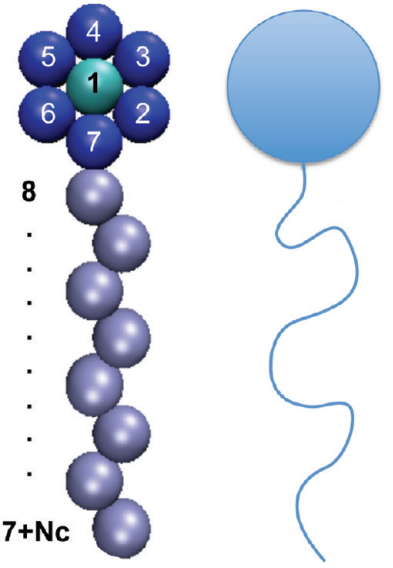

Figure 1. Model of a disk−coil molecule. Blue monomers (2−7) represent the disk periphery and silver monomers (8 to 7+N_c) represent the coil portion, where N_c is the number of coil monomers in one disk−coil molecule. The central monomer (1) of the disk portion is highlighted in green.

Received: May 27, 2011
Revised: August 2, 2011
Published: August 17, 2011

possible.[6] Interestingly, a related system, rod−coil molecules, has received wide attention.[20] Theory in this case has been developed and solved numerically, and it has found good agreement with experiments.[21,22] Furthermore, it was realized in these works that the relative volume fraction of one block to the overall polymer was not the best descriptor, but rather the contour length fractions gave a more intuitive understanding of the underlying physics. This is to be contrasted with the case of coil−coil block copolymers where the volume fraction of one of the blocks is sufficient to describe the system. In this article, we present an exhaustive study of the phase behavior of disk−coil molecules with different coil lengths and different values for the stacking interactions. We construct the phase diagrams for all the different conditions and show that, as in the case of rod−coils, the coil length fraction to the diameter of the disk is a good descriptor. For this system we find a variety of phases depending on the temperature of the system. In particular, we find a disordered phase at high T and a lamellar, perforated lamellar, and cylinder phases with liquidlike correlations at intermediate T depending on the relative strength of the stacking interaction and the length of the coil portion of the molecules. At low temperatures, the disk-rich regions spontaneously order, and we find ordered lamellar, ordered perforated lamellar, and ordered cylinder phases. The appearance of perforated phases is determined by the entropic contribution of the coils that was previously

Table 1. χ_{ij} and r_c^{ij} between Different Types of Monomers i and j

monomer i	monomer j	χ_{ij}	r_c^{ij}
2−7	1−7	1	3.0σ
8−7+N_c	8−7+N_c	0.05(λ)	3.0σ
1−7	8−7+N_c	1	$2^{1/6}\sigma$
1	1	μ	3.0σ

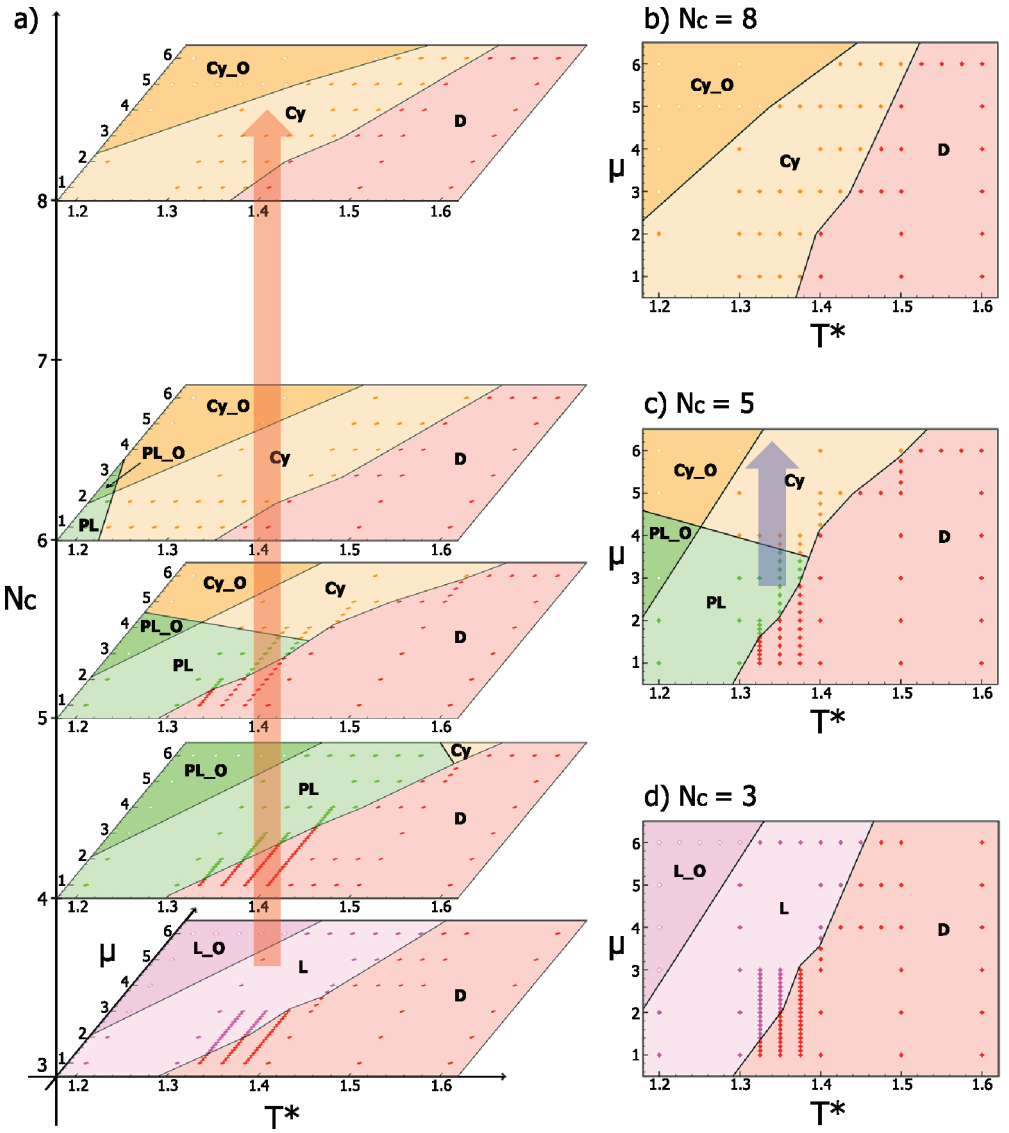

Figure 2. (a) Phase diagram of disk−coil molecules in the T^*, μ, and N_c space. We also present the phase diagrams for fixed N_c as a function of T^* and μ for (b) $N_c = 8$, (c) $N_c = 5$, and (d) $N_c = 3$. D, L, PL, Cy, L_O, PL_O, and Cy_O correspond to disordered, lamellar, perforated lamellar, cylinder, ordered lamellar, ordered perforated lamellar, and ordered cylinder, respectively (see text for explanations). Lines are guidelines for the eye only. The red arrow indicates the direction in which N_c increases, showing the transition path L → PL → Cy. The blue arrow indicates the direction in which μ increases, showing the transition from PL → Cy.

dx.doi.org/10.1021/ma201187p |*Macromolecules* 2011, 44, 7016–7025

measured by the parameter λ[6] and has been observed also in rod−coil systems.[7] In this article we are interested in the experimental regime in which $\lambda \ll 1$, and for the rest of this paper we set it to $\lambda = 0.05$. This corresponds to the relative strength of interaction between alkyl−alkyl groups compared to $\pi-\pi$ stacking interactions.

We study the disk−coil system using a NPT ensemble with the variable cell-shape method.[23,24] Apart from representing the natural conditions of the self-assembly process, this method allows the relaxation of any strain in the system due to the imposed periodic boundary conditions. The simulation box in this method is not fixed, and thus, it relaxes to the natural symmetry of the phase to be assembled. For example, in the case of cylinder phase, the box naturally takes a hexagonal unit cell. Recent work using this method has shown that it is extremely efficient at computing the phase diagram of crystals[25] and block copolymers,[26] and we have found it very useful while studying symmetric disk−coil macromolecules.[6]

The article is organized as follows: Section 2 describes the molecular model and computational details. The complete phase diagram is presented in section 3, where we further explain and analyze each phase. Finally, in section 4 we present our conclusions.

2. MOLECULAR MODEL AND COMPUTATIONAL DETAILS

2.1. Molecular Model. We study the self-assembly of disk−coil molecules having various coil lengths with additional attractive interactions between the central monomers of the disks. These added stacking interactions mimic the extra bonding potential that planar molecules may exhibit in reality. The disk portion of the molecule consists of 7 monomers arranged as a filled and rigid hexagon (numbered 1 to 7), and the coil portion of the molecule consists of N_c monomers (numbered 8 to 7+N_c) (see Figure 1 for a sketch of the molecule). Nearest-neighbor monomers including both coil and disk portions are connected by stiff harmonic springs

$$U(r) = \frac{1}{2}k(r - r_{eq})^2 \tag{1}$$

where $r_{eq} = 2^{1/6}\sigma$ is the equilibrium distance of a Lennard-Jones potential used as the intermolecular potential as explained below and k is a harmonic spring constant. Also, we include additional springs between the following pairs of monomers: (2,5), (3,6), (4,7) to prevent bending or folding of disk. For the springs between the pairs of monomers (2,5), (3,6), (4,7), we use an equilibrium distance of $2r_{eq}$ and a spring constant of $2k$.

The intermolecular potential energy between two monomer types i and j on the macromolecules is described by a typical Lennard-Jones potential with cutoff radius r_c^{ij} for lower computational cost. The general expression for all interactions can be written as

$$U_{LJ}(r_{ij}) = \begin{cases} 4\varepsilon\chi_{ij}\left[\left(\frac{\sigma}{r_{ij}}\right)^{12} - \left(\frac{\sigma}{r_{ij}}\right)^{6} - \left(\frac{\sigma}{r_c^{ij}}\right)^{12} + \left(\frac{\sigma}{r_c^{ij}}\right)^{6}\right] & \text{if } r_{ij} \le r_c^{ij} \\ 0 & \text{otherwise} \end{cases} \tag{2}$$

where, as before, i and j represent the monomer type. In this particular study we have three different types: (i) a coil monomer, (ii) a periphery disk monomer, and (iii) a central disk monomer. The interaction depth $\varepsilon\chi_{ij}$ and the cutoff radius r_c^{ij} depend on the combination of i and j. Table 1 presents the parameters used in this simulations. Notice that ε is the same for all the interactions, and we only vary χ_{ij}.

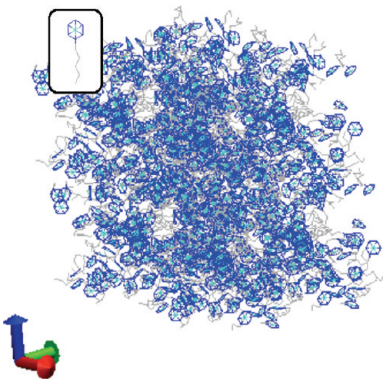

Figure 3. Snapshot of the disordered phase (D) of disk−coil molecules in the wire representation described by lines that connect nearest neighbors. Blue regions represent the disk portion, and gray regions represent the coil portion.

An overview of the interactions is described here. For monomers in the disk periphery (2−7) interacting with other disk beads (1−7) we put $\chi_{ij} = 1$. When considering the interactions between central monomers of the disks (monomer type 1), we set χ_{ij} equal to μ, which can be tuned to induce an additional attractive interaction that prefers parallel stacking of disks. $\mu = 1$ would render all the beads in the disk indistinguishable. The interaction between two monomers in the coil portion, χ_{ij}, is set to 0.05.[27] In this study, the relative attractive potential between coil portions is 20 times weaker than that of disk portions to mimic the real system where the weak attraction between the alkyl chains is substantially lower compared to that from the conjugated parts, as experimental studies have shown. Finally, to allow steric repulsion between disk and coil portions of the molecules, but retain the amphiphilic nature of molecules, we employ an Weeks−Chandler−Andersen (WCA) potential[28] rather than typical Lennard-Jones potential. By using $2^{1/6}\sigma$ as the cutoff radius, the WCA potential only contains the repulsive part of typical Lennard-Jones potential.

2.2. Computational Details. Self-assembly of 128 disk−coil molecules was studied by means of a Metropolis Monte Carlo algorithm. A constant pressure and constant temperature ensemble (NPT) is used with the Parrinello and Rahman box shape method[23,24] to minimize the free energy and remove internal stresses in the system. Periodic boundary conditions in the box shape method are also applied.

For each set of conditions (i.e., temperature, μ, and N_c), we run 10^7 Monte Carlo movement steps to allow the molecules to self-assemble from random initial configurations. Each Monte Carlo step corresponds to a full update of the positions of the molecules; i.e., it corresponds to $128 \times (7 + N_c)$ accepted moves of monomers. At points near phase transitions, where the time to reach equilibrium increases, we run 10^7 additional steps to equilibrate the system. The acceptance ratio of Monte Carlo simulation is adjusted to 0.25 by automatically changing maximum movement distance. The adjusted maximum movement distance is also checked to ensure a high probability to escape

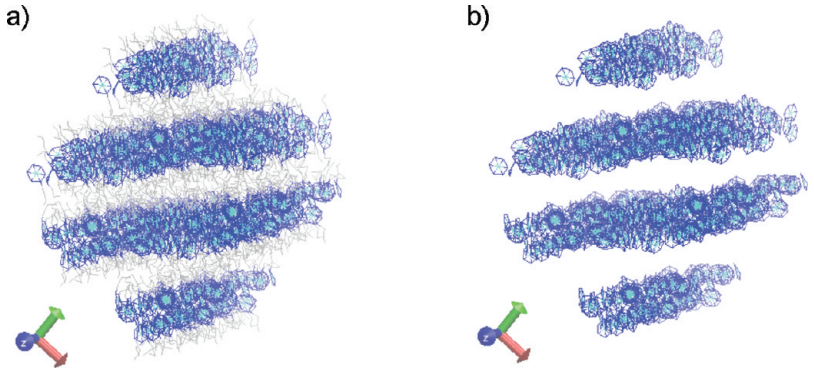

Figure 4. (a) Snapshot of the lamellar (L) phase of disk−coil molecules by using the wire representation. Blue regions represent the disk portion, and gray regions represent the coil portion. In (b) we show only the disks by making the coils transparent, from which one can clearly see the lamellar ordering.

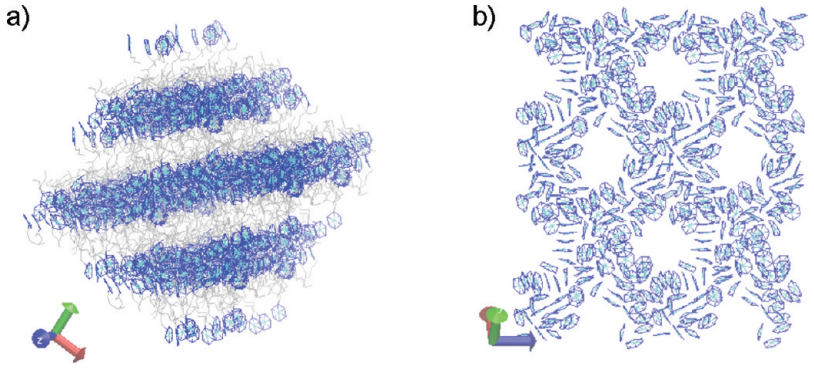

Figure 5. (a) Snapshot of the perforated lamellar phase (PL) of disk−coil molecules by using the wire representation. Blue regions represent the disk portion, and gray regions represent the coil portion. (b) Single disk-rich region picture with transparent coils exhibits a hexagonally close-packed hole array, indicating a perforated lamellar phase.

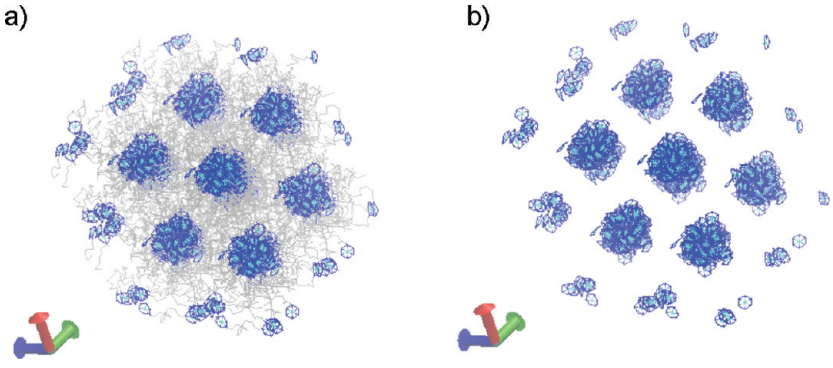

Figure 6. (a) Snapshot of cylinder phase (Cy) of disk−coil molecules by using the wire representation. Blue regions represent the disk portion, and gray regions represent the coil portion. (b) By making the coils transparent, the hexagonally packed cylinders are evident.

form metastable states. Averages are taken over the final 5×10^6 MC steps to study thermodynamic properties.

In this simulation, the role of the coil portion is assumed to be mostly entropic due to the low value of the potential well depth between two monomers in the coil portion (0.05ε). Therefore, by increasing the number of monomers in the coil N_c, we can increase the entropic role of the tail. In contrast, the disk portion contributes mostly in an enthalpic way compared to the coil portion because the potential well between disks is 20 times deeper than that of coils. Also, by adjusting the additional attractive potential μ between central monomers of disks, we control the relative enthalpic role of disks.

Reduced variables are used in this simulation: temperature $T^* = T \times (k_B/\varepsilon)$, distance $r^* = r \times (1/\sigma)$, volume $V^* = V \times (1/\sigma^3)$, pressure $P^* = P \times (\sigma^3/\varepsilon)$, enthalpy $H^* = H \times (1/\varepsilon)$, volume density $\rho^* = \rho$, and spring constant $k^* = k \times (\sigma^2/\varepsilon)$. The

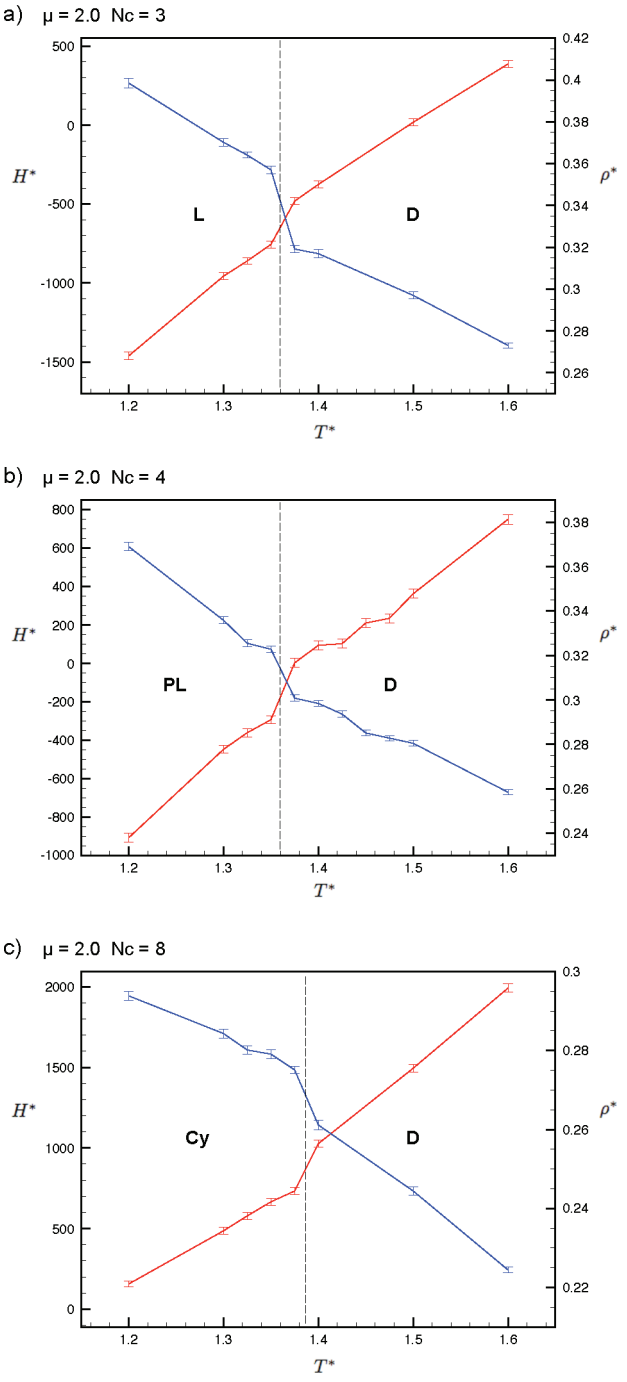

Figure 7. Enthalpy H^* and density ρ^* of the system as a function of the temperature T^* for different values of μ and N_c. The red line represents H^*, and the blue line represents ρ^*. (a) $\mu = 2.0, N_c = 3$; (b) $\mu = 2.0, N_c = 4$; (c) $\mu = 2.0$, $N_c = 8$. The dashed vertical lines represent the transition points.

simulations are performed for a set of reduced temperatures T^* that range from 1.2 to 1.6, and we explicitly study a different set of N_c: 3, 4, 5, 6, and 8. We also change the μ value from 1.0 to 6.0. Also, to prevent the simulation cell from expanding infinitely in the high T^* phases, we imposed a small but finite value of hydrostatic pressure $P^* = 0.1$. We set the spring constant of the harmonic potentials k^* to 2000 and the extra bond spring constant $2k^*$ to 4000.

3. SELF-ASSEMBLED STRUCTURES AND PHASE DIAGRAM OF DISK−COIL MOLECULES

The overall phase diagram of disk−coil macromolecules is shown in Figure 2 as a function of the three relevant parameters, namely the number of monomers in the coil structure N_c, the reduced temperature T^*, and the central monomer interaction parameter μ. In what follows we discuss in detail the different phases obtained.

3.1. Disordered Phase (D). At high temperature, when entropy dominates, disk−coil molecules do not display any particular preferred phase and simply do random Brownian motion. We define this phase as a disordered phase (D) similar to the disordered state in the block copolymer case when the χN parameter is not high enough to allow the system to phase separate. A snapshot of the disordered phase is shown in Figure 3. From the phase diagram in Figure 2, it is also evident that the phase separation temperature from the disordered phase into an ordered state in the disk−coil system is largely controlled by μ. This feature is determined from the fact that the phase transition temperature from D to L, PL, or Cy increases approximately linearly with μ (see Figure 2b−d). This is due to the enthalpic contribution of the disks that grows with the central monomer attractive parameter μ. If the enthalpic part of the free energy of the system from the aggregation of disks exceeds the entropic part of the free energy from fluctuations of the coils and mixing of molecules, the system will phase separate to a lamellar (L), a perforated lamellar (PL), and a cylinder (Cy) phase depending on the coil length N_c, as clearly shown in Figure 2a. Interestingly, we point out that the coil length does not have a large role in determining the order−disorder transition temperature. A large change in N_c from 3 to 8 only yields a minor difference in T_{ODT}.

3.2. Lamellar (L), Perforated Lamellar (PL), and Cylinder (Cy) Phases. Decreasing the temperature from the disordered phase allows the system to phase separate to a lamellar (L), perforated lamellar (PL), and cylinder (Cy) phases. In the lamellar phase, the disk and coil portion order into alternating layers of disk and coil regions, similar to the case of a lipid bilayer. In the perforated lamellar phase, hexagonally close-packed holes exist in the disk-rich region, and these holes are filled with the coils. Finally, the cylinder phase shows hexagonally close-packed disk-rich cylinders surrounded by coils. These features are shown in Figures 4, 5, and 6 for L, PL, and Cy phases, respectively. A discontinuity of the enthalpy H^* and volume density ρ^* as a function of T^* from Figure 7 implies that the phase transition from the disordered state to L, PL, and Cy are all first-order transitions.

The number of monomers in the coil structure of disk−coil molecules plays an important role in determining the phase of the system among the three cases, namely L, PL, and Cy. From Figure 2a, the short coil length $N_c = 3$ of disk−coil molecules drives the system into a L phase which has a relatively lower entropic contribution from the coil compared to the PL and Cy phases. When we increase N_c, the entropy of the coils increases if the volume per single coil is increased since this avoids stretching the chains strongly. Thus, we expect to find other phases by increasing the length of the coil. This is the case, and we find a PL or Cy phase depending on the value of N_c. It is important to note that we observe direct entrance to all of these phases from the disordered phase by changing the length of the coil depending on the value of μ. Furthermore, there are also transitions between the aforementioned phases that depend on the value of μ, and

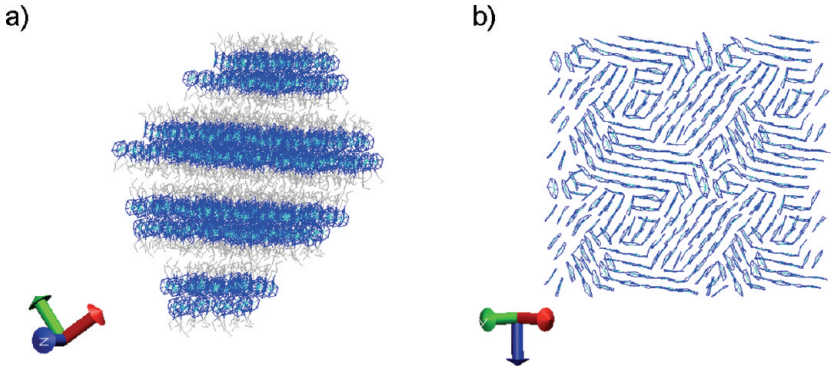

Figure 8. (a) Snapshot of the ordered lamellar phase (L_O) of disk−coil molecules in the wire representation. Blue regions represent the disk portion, and gray regions represent the coil portion. In (b) we present a single layer of disks to examine ordering/stacking of them. The coils have been removed in this figure for visual purposes.

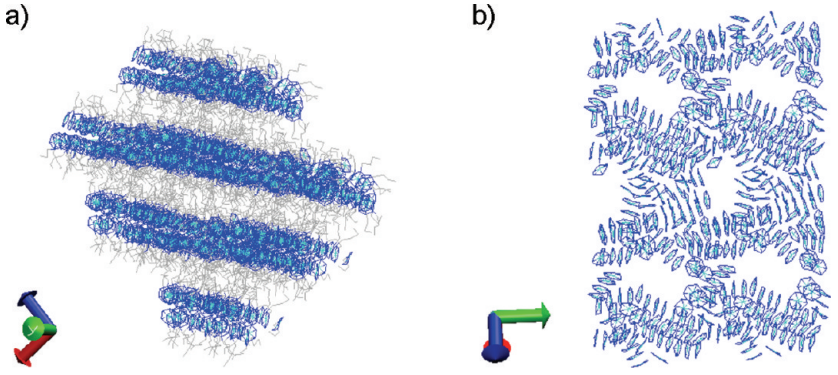

Figure 9. (a) Snapshot of the ordered perforated lamellar phase (PL_O) of disk−coil molecules in the wire representation. Blue regions represent the disk portion, and gray regions represent the coil portion. In (b) we present a single layer of disks to examine ordering/stacking. Notice the appearance of a hexagonally aray of faceted holes. The coil portion is removed in this figure for visual purposes.

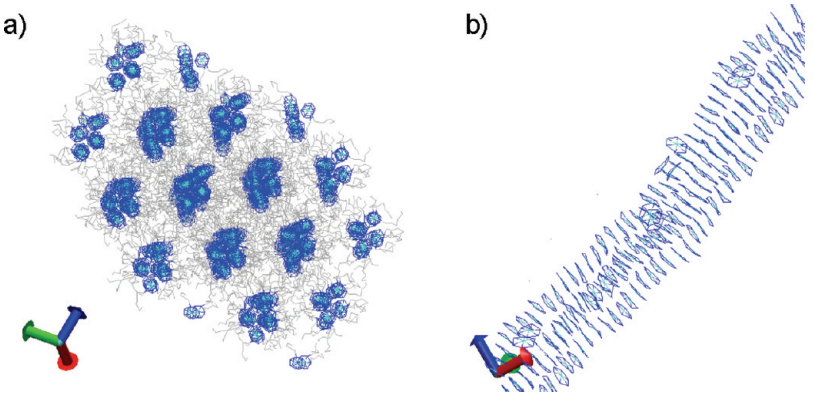

Figure 10. (a) Snapshot of the ordered cylinder phase (Cy_O) of disk−coil molecules in the wire representation. Blue regions represent the disk portion, and gray regions represent the coil portion. In (b) a single disk-rich cylinder is presented to exhibit the high degree of order appearing in the system. The coil portion is removed in this figure for visual purposes.

these can be understood in the same way by noting that increasing the value of μ effectively increases the enthalpic role of the disks.

There are several ways we can navigate through the phase diagram. First, we will consider what happens as we increase the length of the coil N_c, as represented by the vertical transparent red arrow in Figure 2a. At small sizes the L phase is preferred. However, when we increase the length of the coils, the entropy of the coils will drive them to occupy a larger volume by opening holes in the disk-rich region, i.e., the PL phase. As the increase in entropy by opening a hole exceeds the enthalpic loss from the disk-rich region, the free energy of the PL phase becomes lower

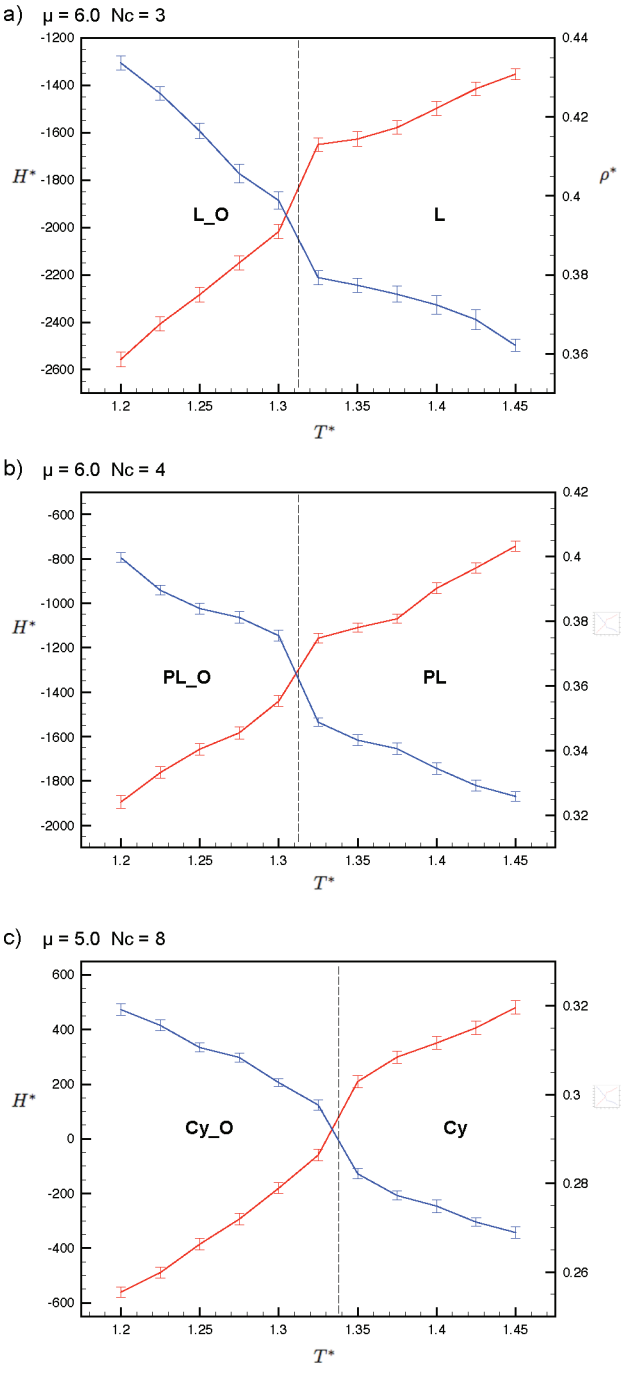

Figure 11. Enthalpy H^* and density ρ^* of the system as a function of the temperature T^* for different values of μ and N_c. The red line represents H^*, and the blue line represents ρ^*. (a) μ = 6.0, N_c = 3; (b) μ = 6.0, N_c = 4; (c) μ = 5.0, N_c = 8. The dashed vertical lines represent the transition points.

than the free energy of L phase, and this results in a stable PL phase. If we further increase N_c, enlarged holes are connected, and the disk region become cylinders surrounded by coils which is the Cy phase. Also, these cylinders are hexagonally close-packed in a coil-rich matrix to minimize the free energy of the system.

Even though the sequence L → PL → Cy transition can be observed by increasing N_c, we can also control the relative entropic role of the coils by changing μ, as stated before. Using this variable instead, we can move in the phase diagram by following the transparent blue arrow in Figure 2c. Higher μ values increase the effective enthalpic role of the disks, while the entropy contribution of the coils remains the same. Thus, in relative fashion, at larger μ the coils are more "entropic" in the high-μ region. This explains why one goes from a PL → Cy phase. We can clearly see this feature in Figure 2c.

3.3. Ordered Lamellar (L_O), Ordered Perforated Lamellar (PL_O), and Ordered Cylinder (Cy_O) Phases. From the L, PL, and Cy phases, if we further decrease the temperature or increase the μ, the system crystallizes to an ordered lamellar (L_O), ordered perforated lamellar (PL_O), and ordered cylinder (Cy_O) phases. These phase transitions are also first order from the discontinuity of H^* and ρ^* as a function of T^*, as shown in Figure 11. Snapshots of L_O, PL_O, and Cy_O phases are shown in Figures 8, 9, and 10, respectively. L_O, PL_O, and Cy_O phases have the same large scale structure as their fluid couterparts L, PL, and Cy phases, respectively, but the disks are ordered in specific ways in the ordered phases. In the L_O phase, trains of disks composed of 3−5 stacked disks in parallel are close-packed to form a disk-rich region with lamellar symmetry. Similarly, the PL_O phase contains similar trains of disks forming the disk-rich region, except for the fact that there exist also holes in the disk-rich region. In the Cy_O phase, most disks are stacked in parallel, and three or four of these long trains aggregate to form a columnar structure similar to that appearing in discotic liquid crystals.

To study the parallel stacking of disks quantitatively, we define an order parameter that integrates the short-range part of the radial distribution function of the central monomers in the disks, mathematically written as

$$P_{\text{parallel}} = \int_0^{1.5r_{\text{eq}}^*} g(r^*)4\pi r^{*2}\, dr^* \tag{3}$$

where $g(r^*)$ is the radial distribution function of the central bead of disks, namely monomer 1. This order parameter is the average number of stacked disks in parallel and can vary from 0 to 2. The latter value is obtained when every disk is stacked in parallel in an idealized fashion. P_{parallel} values for L_O, PL_O, and Cy_O phases under all sets of conditions (T^*, μ, N_c) were calculated and are listed in Table 2.

Table 2 shows that P_{parallel} values stay in the range from 1.35 to 1.5 for PL_O and L_O phases, but jump to values around 1.8 at the Cy_O phase, clearly indicating the preferred alignment in this microstructure. Another useful function to quantify the ordering of disks is the average number of stacked disks in a row N_{parallel} that can be calculated roughly from P_{parallel} as follows:

$$N_{\text{parallel}} = \frac{2}{2 - P_{\text{parallel}}} \tag{4}$$

This equation is obtained by noting that the average number of parallel stacked neighbors in a given ordered train of N_{parallel} molecules can be written as $P_{\text{parallel}} = (2N_{\text{parallel}} - 2)/N_{\text{parallel}}$. This equation is intuitive, since the total number of parallel stacked neighbors is $2N_{\text{parallel}} - 2$, where the last subtraction accounts for the ends. Finally, to obtain the average, we need to divide by the total number of molecules in the train N_{parallel}.

Calculated N_{parallel} values for L_O and PL_O phases range from 3.08 to 4.0 which are similar in range to what is observed directly by visual inspection. From Figures 8b and 9b, we can

Table 2. $P_{parallel}$ Values for Different Simulation Conditions (T^*, μ, N_c) Corresponding to L_O, PL_O, or PL_O Phases

T^*, μ, N_c	phase	$P_{parallel}$	T^*, μ, N_c	phase	$P_{parallel}$	T^*, μ, N_c	phase	$P_{parallel}$
1.2, 3.0, 3	L_O	1.463	1.2, 4.0, 3	L_O	1.451	1.2, 5.0, 3	L_O	1.396
1.2, 6.0, 3	L_O	1.480	1.3, 6.0, 3	L_O	1.472	1.225, 6.0, 3	L_O	1.455
1.25, 6.0, 3	L_O	1.486	1.275, 6.0, 3	L_O	1.383	1.2, 3.0, 4	PL_O	1.406
1.2, 4.0, 4	PL_O	1.463	1.2, 5.0, 4	PL_O	1.465	1.2, 6.0, 4	PL_O	1.473
1.3, 6.0, 4	PL_O	1.479	1.225, 6.0, 4	PL_O	1.433	1.25, 6.0, 4	PL_O	1.425
1.275, 6.0, 4	PL_O	1.476	1.2, 3.0, 5	PL_O	1.439	1.2, 4.0, 5	PL_O	1.370
1.2, 5.0, 5	Cy_O	1.798	1.2, 6.0, 5	Cy_O	1.779	1.3, 6.0, 5	Cy_O	1.802
1.2, 3.0, 6	Cy_O	1.815	1.2, 4.0, 6	Cy_O	1.782	1.2, 5.0, 6	Cy_O	1.833
1.2, 6.0, 6	Cy_O	1.870	1.3, 5.0, 6	Cy_O	1.801	1.3, 6.0, 6	Cy_O	1.797
1.2, 3.0, 8	Cy_O	1.798	1.2, 4.0, 8	Cy_O	1.833	1.2, 5.0, 8	Cy_O	1.784
1.2, 6.0, 8	Cy_O	1.827	1.3, 5.0, 8	Cy_O	1.816	1.3, 6.0, 8	Cy_O	1.795
1.325, 5.0, 8	Cy_O	1.855	1.4, 6.0, 8	Cy_O	1.826	1.225, 5.0, 8	Cy_O	1.799
1.25, 5.0, 8	Cy_O	1.817	1.275, 5.0, 8	Cy_O	1.832			

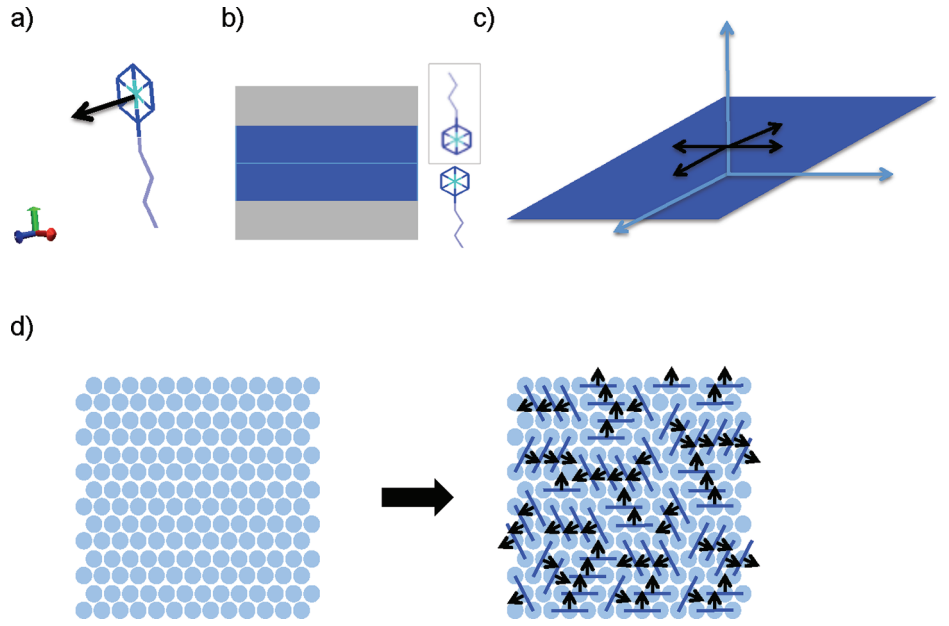

Figure 12. (a) Description of the director vector for a disk−coil macromolecule. (b) Two-dimensional structure induced due to the presence of coils in L_O and PL_O phases that has two degrees of freedom for director vector, as shown in (c). (d) Hexagonal arrangement of the director is achieved when disks are close-packed in the disk-rich layer.

clearly see that trains composed of 3−5 stacked disks in parallel are close-packed to form disk-rich layers. However, for the Cy_O phase, the calculated $N_{parallel}$ value reaches 10.0, which means disks are highly ordered. After counting some defects, 12−15 disks stacked in parallel should be observable, and this is clearly seen in Figure 10.

From our quantitative studies on the parallel stacking of disks, we can conclude that the coil structure in the disk−coil molecule plays a critical role in the ordering of disks. Increasing the number of monomers N_c increases the entropy of the system and allows it to transform from L_O phase to PL_O phase. A further increment of N_c drives the system to reach a Cy_O phase from a PL_O phase, which is accompanied by an enhanced parallel order of the disks. We can explain this enhancement in the order by analyzing the director field under confinement. The director vector is defined as the unit vector normal to the plane of a disk as described in Figure 12a. For a two-dimensional periodic structure such as the L_O or the PL_O phases, the director vector has two degrees of freedom as shown in Figure 12b,c. In these crystalline phases (low T^*), the only way to stack disks in a close-packed manner is a 6-fold degenerate hexagonal arrangement.[6] However, when we include the stacking interactions, the degeneracy is lifted, and the L_O and PL_O phases contain close-packed short trains composed of 3−5 disks stacked in parallel (see Figure 12d). We note, however, that the number of parallel stacked molecules is not very high because a single stacked "column" is unstable to the appearance of "excited" states that correspond to defects in the stacking profile, where a defect is a disk with a director vector misaligned with the train. Although there is an energetic cost for introducing these defects, it is sufficiently small that thermal fluctuations give rise to these defects. The major energetic cost is not in the lateral interactions

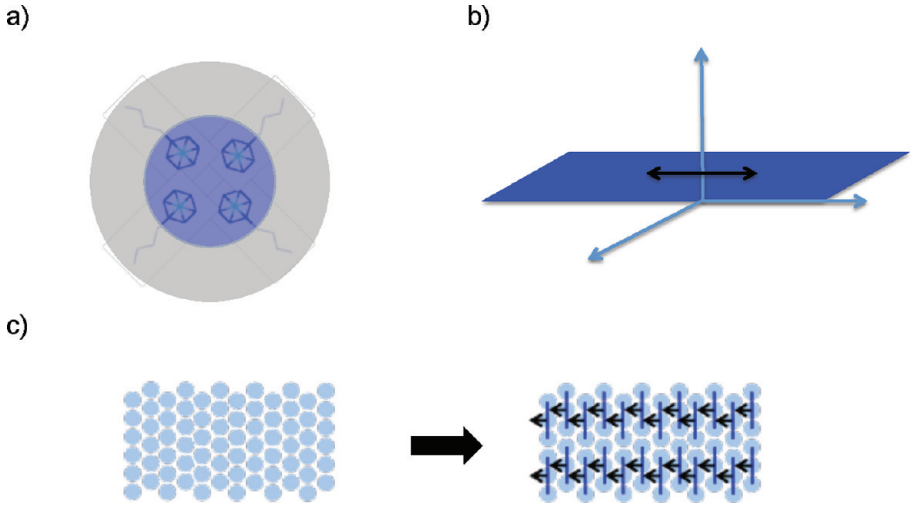

Figure 13. (a) Cylinder structure induced by long polymer tails compared to disk size. (b) In this case (Cy_O phase) only one degree of freedom exists for director vector. (c) Parallel alignment of the director is achieved when disks are close-packed and stacked on top of each other in disk-rich cylinder.

because the periphery disk beads do not interact differently between themselves and the central monomers and hence emerges only from the misalignment of the director vector and corresponding loss of favorable stacking interactions. Thus, what we have in reality is an one-dimensional problem that corresponds essentially to an 1D Ising model, where the two "spins" correspond to director vectors that are either aligned with the stack or misaligned with the stack. It is well-known that an 1D Ising model of this type is unstable, giving rise to short stacks. This remains true for the cylinder case, but the difference in the defect energies is greatly enlarged in the Cy phase for the following reason: in the Cy_O phase inserting a "defect" across a cylinder implies that one has to bring into contact coil molecules with disk monomers, and this is highly energetically unfavorable. As a result, in the Cy_O phase, the director field is confined to one dimension, and thus, the disks stack in parallel (see Figure 13a,b). This enhances the long-range parallel ordering of disks in the Cy_O phase as described in Figure 13c. In summary, confinement of the disks due to microphase separation that can be controlled by the length of the coils has a huge effect in the final arrangement of the disks in assemblies of disk−coil macromolecules.

4. CONCLUSIONS

In this article we explored the phase behavior of disk−coil molecule lengths using Monte Carlo simulations. We constructed a comprehensive phase diagram as a function of temperature T^* as well as two tunable properties that depend on the chemistry, namely the stacking interaction parameter μ and the number of monomers in the coil N_c. At intermediate temperatures ranging from $T^* = 1.3$ to $T^* = 1.5$, L, PL, and Cy phases appear depending on T^* and N_c. Increasing μ helps the system to phase separate at higher temperature due to the large enthalpic contribution of the disks. Also, by increasing N_c, the system phase transforms from L phase to PL phase, and further increasing N_c drives the system to transform to Cy phase. The PL → Cy transformation can also be achieved by increasing μ. Further decreasing T^* or increasing μ yields crystalline disk phases denoted as L_O, PL_O, and Cy_O. These ordered phases contain disks stacked in parallel with a variable degree of ordering. To study the parallel stacking in a quantitative fashion, we used the average number of parallel stacked disks per molecule $P_{parallel}$. From this quantity we could calculate $N_{parallel}$, the average number of stacked disks in a row. On the basis of $N_{parallel}$, 3−5 stacked disks are close-packed in the lamellar or perforated lamellar phases. However, $N_{parallel} \sim 12-15$ in the Cy_O phase. We can explain this difference based on the different degree of a confinement in each structure. In conclusion, our results reveal the phase behavior of disk−coil macromolecules and provide new design strategies to control the order of planar macromolecules. Compared to previous studies of disk−coil molecules that just considered a single coil length,[6] the present work shows two different routes to achieve a particular morphology. This can be done by either modifying the chemistry of the disk part to increase or decrease the stacking interaction parameter or changing the length of the coil. In previous studies the latter had been held fixed, but as shown here, it is very important in determining the final morphology. This is something that is well accepted in the self-assembly of block copolymer phases but is not so widely appreciated in the field of supramolecular chemistry. A particular example of this is the two longest coils studied here ($N_c = 6, 8$), where the system, even without added stacking interactions ($\mu = 1$), self-assembles into a cylinder phase. This had not been observed in previous studies.[6] Finally, the thermodynamics of disk−coil macromolecules provide important insight into the self-assembly of chlorophyll molecules which have a planar disk and single coil structure. In particular, by controlling the coil length, one can induce two-dimensional or one-dimensional confined disks, which in turns strongly dictates the degree of stacking.

AUTHOR INFORMATION

Corresponding Author

*E-mail: aalexand@mit.edu.

ACKNOWLEDGMENT

This work would have not been possible without the funding kindly provided by a MIT Energy Initiative Seed Grant, by the MRSEC Program of the National Science Foundation under Award DMR-0819762, and by a STX fellowship.

REFERENCES

(1) Adam, D.; Schuhmacher, P.; Simmerer, J.; Haussling, L.; Siemensmeyer, K.; Etzbach, K. H.; Ringsdorf, H.; Haarer, D. *Nature* **1994**, *371*, 141.

(2) Boden, N.; Bushby, R. J.; Clements, J.; Movaghar, B. *J. Mater. Chem.* **1999**, *9*, 2081.

(3) Nahor, G. S.; Mosseri, S.; Neta, P.; Harriman, A. *J. Chem. Phys.* **1988**, *92*, 4499.

(4) Naruta, Y.; Sasayama, M.; Sasaki, T. *Angew. Chem., Int. Ed.* **1994**, *33*, 1839.

(5) Schmidt-Mende, L.; Fechtenkotter, A.; Mullen, K.; Moons, E.; Friend, R. H.; MacKenzie, J. D. *Science* **2001**, *293*, 1119.

(6) Kim, Y.; Alexander-Katz, A. *J. Chem. Phys.* **2010**, *132*, 174901. Kim, Y.; Alexander-Katz, A. *J. Chem. Phys.* **2011**, *135*, 024902.

(7) Horsch, M. A.; Zhang, Z.; Glotzer, S. C. *Phys. Rev. Lett.* **2005**, *95*, 056105.

(8) Wu, D.; Zhi, L.; Bodwell, G. J.; Gui, G.; Tsao, N.; Mullen, K. *Angew. Chem., Int. Ed.* **2007**, *46*, 5417.

(9) Wu, D.; Pisula, W.; Enkelmann, V.; Feng, X.; Mullen, K. *J. Am. Chem. Soc.* **2009**, *131*, 9620.

(10) Staehelin, L. A.; Golecki, J. R.; Drews, G. *Biochim. Biophys. Acta* **1980**, *589*, 20.

(11) Psencik, J.; Ikonen, T. P.; Laurinmaki, P.; Merckel, M. C.; Butcher, S. J.; Serimaa, R. E.; Tuma, R. *Biophys. J.* **2004**, *87*, 1165.

(12) Oostergetel, G. T.; Reus, M.; Chew, A. G. M.; Bryant, D. A.; Boekema, E. J.; Holzwarth, A. R. *FEBS Lett.* **2007**, *581*, 5435.

(13) Jochum, T.; Reddy, C. M.; Eichhofer, A.; Buth, G.; Szmytkowski, J.; Kalt, H.; Moss, D.; Balaban, T. S. *Proc. Natl. Acad. Sci. U.S.A.* **2008**, *105*, 12736.

(14) Ganapathy, S.; Oostergetel, G. T.; Wawrzyniak, P. K.; Reus, M.; Chew, A. G. M.; Buda, F.; Boekema, E. J.; Bryant, D. A.; Holzwarth, A. R.; de Groot, H. J. M. *Proc. Natl. Acad. Sci. U.S.A.* **2009**, *106*, 8535.

(15) Andrienko, D.; Marcon, V.; Kremer, K. *J. Chem. Phys.* **2006**, *125*, 124902.

(16) Veerman, J. A. C.; Frenkel, D. *Phy. Rev. A* **1992**, *45*, 5632.

(17) Bates, M. A.; Luckhurst, G. R. *J. Chem. Phys.* **1996**, *104*, 6696.

(18) Caprion, D.; Bellier-Castella, L.; Ryckaert, J.-P. *Phys. Rev. E* **2003**, *67*, 041703.

(19) Zhang, Z.; Horsch, M. A.; Lamm, M. H.; Glotzer, S. C. *Nano Lett.* **2003**, *3*, 1341.

(20) Lee, M.; Cho, B. K.; Zin, W. C. *Chem. Rev.* **2001**, *101*, 3869.

(21) Pryamisyn, V.; Ganesan, V. *J. Chem. Phys.* **2004**, *120*, 5824.

(22) Olsen, B. D.; Shah, M.; Ganesan, V.; Segalman, R. A. *Macromolecules* **2008**, *41*, 6809.

(23) Parrinello, M.; Rahman, A. *J. Appl. Phys.* **1981**, *52*, 7182.

(24) Ray, J. R.; Rahman, A. *J. Chem. Phys.* **1984**, *80*, 4423.

(25) Filion, L.; Marechal, M.; van Oorschot, B.; Pelt, D.; Smallenburg, F.; Dijkstra, M. *Phys. Rev. Lett.* **2009**, *103*, 188302.

(26) Barrat, J.-L.; Fredrickson, G. H.; Sides, S. W. *J. Phys. Chem. B* **2005**, *109*, 6694.

(27) Increasing the interaction from the tails leads to the disappearance of the perforated lamellar phase for uniform disks, i.e., $\mu = 1$ as shown in ref 6. We expect that for larger values of μ the same trend will persist.

(28) Weeks, J. D.; Chandler, D.; Andersen, H. C. *J. Chem. Phys.* **1971**, *54*, 5237.